Supplementary Methods

All studies were conducted according to approved Institutional Review Boards (IRBs) protocols at the Cleveland Clinic and University Hospitals–Cleveland Medical Center. We recruited pediatric and young adult subjects with a clinical and/or genetic diagnosis of ARPKD (n=13), age ≥6 years, eGFR>30ml/min/1.73m^2, no prior organ transplant and no contraindications for MRI scanning. Of the thirteen subjects with a diagnosis of ARPKD, eleven had previous genetic testing, confirming biallelic pathogenic variants in the PKHD1 gene. Of the two subjects diagnosed on clinical criteria, both had highly suggestive presentation in infancy with typical kidney imaging findings as well as kidney and/or liver tissue pathology in affected siblings or the patient themselves. Serum creatinine and cystatin C were obtained to estimate GFR using the CKID U25 formula.[S1] Proteinuria was assessed by spot urine total protein to creatinine measurements. Healthy young adult volunteers (n=8) with no known kidney disease were also recruited for comparison. No clinical data were obtained for the volunteers.

Each ARPKD patient and volunteer was scanned supine in a Siemens 3T MRI scanner with the same MRI protocol consisting of three primary components: 1) rapid, localizer scans to enable accurate slice positioning for the subsequent kidney scans; 2) a previously-described kidney MRF method to generate co-registered coronal kidney T_1 and T_2 maps during 15-second breath-holds (3 coronal slices near the renal hilum, field of view = 400 mm, matrix size = 256 x 256, slice thickness = 5 mm, scan time = 15 seconds / imaging slice, scans acquired during manual breath-holds);[S2] 3) a respiratory-triggered non-contrast pseudo-continuous arterial spin labeling MRI method to measure kidney cortical perfusion (ASL, field of view = 300 x 150 mm, matrix size = 64 x 32, slice thickness = 6 mm, number of signal averages = 20).[S3] Note that one of the ARPKD patients was not able to complete the ASL MRI scan, but this subject did complete the MRF scan. All other ARPKD subjects and volunteers completed both the MRF and ASL scans.

None of the patients were sedated for the kidney MRI scans, and both chest and spine array coil were used to acquire the MRI data.

The kidney MRF data and the ASL perfusion data were exported for offline reconstruction in Matlab (R2019a; MathWorks, Natick, MA). To calculate mean T_1, T_2, and perfusion values for each subject, regions-of-interest (ROIs) were manually selected covering the entire left and right kidneys in each imaging slice. Note that separate cortical and medullary assessments were obviated for the ARPKD patients as the diffuse cysts covered the majority of each subject's kidneys. For the perfusion analysis, a thresholding analysis was performed after the kidney ROI selection on the kidney perfusion maps to select the kidney cortex in each imaging slice to specifically assess kidney cortical perfusion. The image analysis was performed on each dataset by two skilled raters (all raters: C.J.M., M.P.-G., M.E.K., Y.Z.), and the results were compared for consistency (<5% difference between raters) prior to averaging the results between the raters. Mean kidney T_1, T_2 values were obtained for each kidney by calculated a weighted average of the results across all imaging slices. Each slice was weighted by the number of voxels in each slice. The perfusion assessments were obtained in one central slice. The final overall average was calculated by averaging across the left and right kidneys and all raters.

Statistical Analysis

Non-parametric Wilcoxon rank sum tests were performed to compare the kidney MRI and eGFR data between all the subjects with ARPKD (n=13) and the healthy volunteers (n=8). In a secondary analysis, the ARPKD subgroups with either early CKD or mild-moderate CKD were also compared with non-parametric Wilcoxon rank sum tests. All tests were two-tailed and performed at a significance level of 0.05.

Supplementary Results
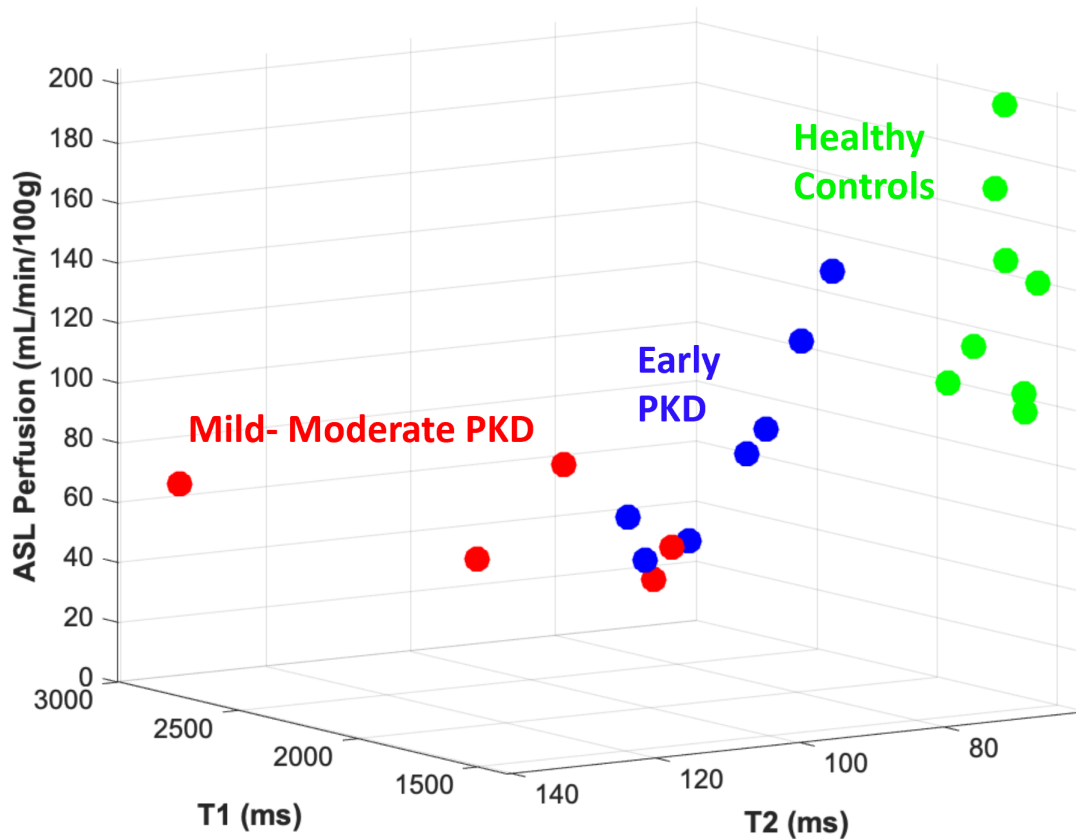
Supplementary Figure S1. 3D Visualization of Multi-Modal MRI Assessments in ARPKD Patients and Adult Healthy Volunteers

A 3D visualization showing distinct stratification among ARPKD patients with early CKD (blue circles), mild-moderate CKD (red circles), and healthy volunteers (green circles). Results from 12 of the 13 ARPKD patients enrolled in the study are shown in the 3D plot, as the ASL scan was not completed for one of the ARPKD patients (eGFR=81 ml/min/1.73m^2).
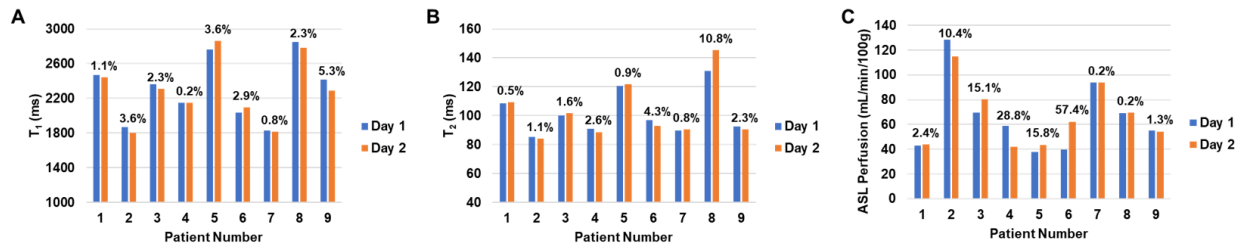
Supplementary Figure S2. Repeatability of MRI Assessments

Repeatability plots of mean kidney T_1 (**A**), T_2 (**B**), and perfusion (**C**) from 9 ARPKD patients scanned on consecutive days. The percent difference in the biomarker between the scans conducted on Day 1 (in blue) and Day 2 (in orange) are shown for each patient.

Supplemental References

S1. Pierce CB, Muñoz A, Ng DK, Warady BA, Furth SL, Schwartz GJ. Age- and sex-dependent clinical equations to estimate glomerular filtration rates in children and young adults with chronic kidney disease. *Kidney Int*. 2021;99:948–956.

S2. MacAskill CJ, Markley M, Farr S, Parsons A, Perino JR, McBennett K, Kutney K, Drumm ML, Pritts N, Griswold MA, Ma D, Dell KM, Flask CA, Chen Y. Rapid B1-Insensitive MR Fingerprinting for Quantitative Kidney Imaging. *Radiology*. 2021;300:380–387.

S3. Alhummiany BA, Shelley D, Saysell M, Olaru M-A, Kühn B, Buckley DL, Bailey J, Wroe K, Coupland C, Mansfield MW, Sourbron SP, Sharma K. Bias and Precision in Magnetic Resonance Imaging-Based Estimates of Renal Blood Flow: Assessment by Triangulation. *J Magn Reson Imaging*. 2022;55:1241–1250.